Diffusive dynamics on paper matrix

Kaustav Chaudhury [1], Shantimoy Kar [2], and Suman Chakraborty [1, 2*]

[1] Department of Mechanical Engineering, Indian Institute of Technology Kharagpur, Kharagpur – 721302, India

[2] Advancement Technology Development Centre, Indian Institute of Technology Kharagpur, Kharagpur – 721302, India

[*] Corresponding author, email: suman@mech.iitkgp.ernet.in

ABSTRACT

Writing with ink on paper and rapid diagnostics of diseases using paper cartridge, despite their remarkable diversities from application perspective, both involve the motion of a liquid from a source on porous hydrophilic substrate. Here, we bring out a generalization in the pertinent dynamics, by appealing to the concerned ensemble-averaged transport, with reference to the underlying molecular picture. Our results reveal that notwithstanding the associated complexities and diversities, the resultant liquid transport characteristics on paper matrix, in a wide variety of applications, resemble universal diffusive dynamics. Agreement with experimental results from diversified applications is generic, and validates our unified theory.

Keywords: Paper microfluidics, microcapillary, random motion, diffusive dynamics, porous material

MAIN TEXT

From the dawn of modern civilization, writing on a piece of paper with an ink has been one of the preferred modalities of transferring knowledge and information in documented form, from one generation to other [1,2]. On a different note, beginning of this century has witnessed another emerging prospect of a paper matrix: acting as the essential building block of a rapid diagnostic kit for testing blood, urine, and saliva samples in ultra-low-cost paradigm [3–5]. Such apparently diversified applications of spreading hydrodynamics across a paper matrix are all attributable to the remarkable transport characteristics through the topographically complicated fibrous networks constituting a paper [6–9]. Despite the fact that capillary imbibition and transport on porous substrates have been studied for decades, any unified understanding on how liquid transports on a paper, remains elusive. In the literature, various models have been put forward to explain the underlying physical phenomena [6–12]. However, most of these models are complex and problem-specific in nature, with conflicting implications at occasions. This deficit stems from the complexities in generalizing the underlying physics through a simplified paradigm, amidst the diversities in the pertinent applications.

Here, we unveil universal diffusive characteristics of liquid transport on a paper matrix, notwithstanding the underlying diversities hallmarked by the requirements of specific applications. By mapping the single micro-capillary flow behavior onto the spatially distributed network through the ensemble orientation characteristics of the constituent fibers, we effectively draw an analogy with the diffusion due to complex migration characteristics of molecules or particles [13–15]. This culminates in effective diffusive transport behavior on paper, brought about propelling of liquid through the spatially oriented tortuous fiber network. Resolving the apparent anomalies in various models describing transport phenomena on a paper matrix in case-specific scenarios, our conceptual paradigm appears to bring in a generalization by providing a simple and consistent accounting of notable reported observations ranging from liquid imbibitions, mixing and separation, to the hydrodynamics of writing.

We first depict a representative scanning electron micrograph of the distributions of the capillaries in a paper (Fig. 1, analyzed for Whatmann grade 1 filter paper). The micrograph shows random distribution of the capillaries. A quantitative depiction of

the orientation and distribution of the constituent capillaries in a paper matrix can be ascribed through the orientation angle of each capillary with respect to a fixed datum [16]. In particular, the standard deviation of the orientation angles connotes the resultant distribution of the capillaries. This fundamental understanding is the key essence in mathematical representation of the spatial distribution of the fibers in various substances ranging from near-isotropic, machine direction oriented and unidirectional media [16]. The near isotropic distribution is characterized by the high magnitude of the standard deviation of the orientation angles (typically greater than 40^{o} [16]).

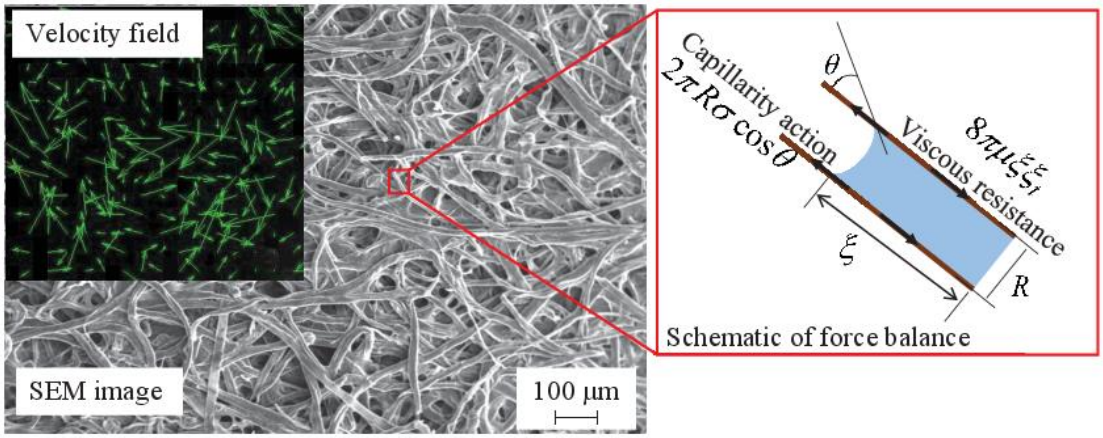

Fig. 1. Random porous matrix of Whatman filter paper (grade 1). Scanning electron micrograph (SEM) shows the distribution of the pores. The velocity field (in-plane) during a liquid flow through these pores, obtained from micro-particle image velocimetry (μ-PIV), is shown in the inset. Details of the μ-PIV analysis considered in the present study are provided in the supplementary document. The length estimate shown here is for the SEM image. A schematic of the force distribution on each pore, forming the basis for the present analysis, is shown for a representative sample.

The micrographic structure of Whatmann filter paper (grade 1), as shown in Fig. 1, has standard deviation of 67^{o} for the orientation angels of the constituent capillaries. Thus, quantitatively, we can consider the capillary distribution as near-isotropic [17]. Such typical capillaries find applications in microscale analytical devices and writing platforms. The randomness in the liquid motion is also apparent from the velocity distribution during liquid flow through paper matrix (cf. μPIV image in Fig. 1).

Amidst the ensemble network of the capillaries composing the paper, let us consider a single capillary with hydraulic radius R. Let ξ denote the displacement of the liquid column within this capillary. The liquid transport dynamics within the

sample capillary can be described by the force balance equation (see also Fig. 1): $\left(\rho\pi R^2\xi\xi_t\right)_t = 2\pi R\sigma\cos\theta - 8\pi\mu\xi\xi_t$, where ρ is the density, μ is the viscosity, σ is the liquid-air surface tension, and θ is a dynamically evolving contact angle. The subscript t represents derivative with respect to time t. Here, the right hand side is the resultant force, which is a combined consequence of driving interfacial tension and retarding viscous resistance. The liquid transport equation can be recast as $\left(\xi\xi_t\right)_t = u^* - \xi\xi_t/\tau^*$, where $\tau^* = \rho R^2/8\mu$ and $u^* = \left(2\sigma\cos\theta/\rho R\right)$. Here $\xi\xi_t/\tau^*$ describes the viscous dissipation with τ^* being the characteristic time scale for viscous diffusion of momentum, and u^* accounts for the work (per unit mass) required to carry out the liquid transport. As a consequence, liquid transport dynamics is governed by the rate of energy change $\left(\xi\xi_t\right)_t$ in the system.

The average pore size of the capillaries constituting a paper usually varies from around 10^{-3} to 10^{1} microns [18,19]. Over such length scales, molecular scale interactions are likely to offer significant impact into the underlying transport [20–26]. Molecules of liquid, air and the capillary surface constitute the vicinity of the moving contact-line in a capillary. However, due to the intermittent motions of the molecules, molecular exchange between the species takes place which can be characterized by the frequency κ and the length λ of a displacement. From molecular viewpoint [24,27], the wetting process can be viewed as an activated rate process governed by the theories of reaction rates, resulting from the intermittent molecular jumps. The work done by the surface tension force, proportional to $\sigma\left(\cos\theta_0 - \cos\theta\right)$, with θ_0 being the equilibrium contact angle, results in the disturbance of the wetting equilibrium, leading to the contact-line motion [24,27] $\xi_t = = 2\lambda\kappa^0\sinh\left[\left(\sigma/2nk_BT\right)\left(\cos\theta_0 - \cos\theta\right)\right]$, where n is the number (per unit area) of sites on the capillary wall at which molecules are adsorbed while jumping with effective jump displacement λ and equilibrium jump frequency κ^0. The other parameters include: Boltzmann constant k_B and temperature T. Comprehensive details are provided in the accompanying supplementary document.

We next ensemble average the capillary transport equation. The resultant equation reads as $\left\langle\left(\xi\xi_t\right)_t\right\rangle = \left\langle u^*\right\rangle - \left\langle\xi\xi_t/\tau^*\right\rangle$. In this case $\left\langle u^*\right\rangle = \left\langle\left(2\sigma/\rho R\right)\cos\theta_0\right\rangle -$

$\left\langle \left(4nk_BT/\rho R\right)\sinh^{-1}\left(\xi_t/2\kappa^0\lambda\right)\right\rangle$, and $\left\langle \xi\xi_t/\tau^*\right\rangle = \left\langle \xi\xi_t\right\rangle\left\langle \tau^{*-1}\right\rangle$. Here, we consider $R_{avg}=\left\langle R\right\rangle$, as the average pore size of the capillaries constituting the paper matrix. From our micro-particle-image-velocimetry (μPIV) based scrutiny (Fig. 1), it is evident from the random velocity field that the liquid has equal probability to move in any direction through the isotropically distributed capillaries constituting the paper matrix. Thus, without any loss of generality, one can consider $\left\langle \xi_t\right\rangle = 0$. We further note $\xi\xi_t = 2^{-1}\left(\xi^2\right)_t$, leading to $\left\langle \xi\xi_t\right\rangle = 2^{-1}\left\langle \left(\xi^2\right)_t\right\rangle = 2^{-1}\left(\left\langle \xi^2\right\rangle\right)_t$, where $\left\langle \xi^2\right\rangle$ describes the mean square displacement. The ensemble average operation finally yields $\psi_{tt} = u - \psi_t\tau^{-1}$ where $\psi = \left\langle \xi^2\right\rangle$ describes the mean square displacement. The other factors read as $u = \left(2\sigma/\rho R_{avg}\right)\cos\theta_0$, and $\tau = \rho R_{avg}^2/8\mu$. The above differential equation has an analytical solution: $\left\langle \xi^2\right\rangle = 2u\tau^2\left[\left(t/\tau\right)-1+\exp\left(-t/\tau\right)\right]$.

It is important to mention that the above analytical form bears a similarity with the equation describing the liquid front propagation dynamics within a capillary [28]. While the reported study [28] unveils the subtleties of liquid filling dynamics through a single capillary, the present analysis describes the ensemble behavior of the liquid spreading through the randomly distributed multiple capillaries. Therefore, despite the apparent similarities, there is a striking difference in the physical consequences between the present and the reported study [28]. This critical aspect can be appreciated from the analysis of liquid propagation dynamics at different time scales.

For liquid filling through a single capillary, one can obtain an inertial or inviscid regime and viscous or the celebrated Bell-Cameron-Lucas-Washburn (BCLW) regime of operation [29]. The consequent demarcation is with respect to the viscous and capillary time scales. In particular, the BCLW regime is hallmarked by the balance of viscous and capillary forces in which the operating time is of the order of the viscous time scale, observed at the late stage of the filling event [29]. At early stage, however, the inertial effect dominates over the viscous effect and the former is balanced by the capillary force. The corresponding time scale characterizing this regime is the inertial-capillary time scale [29].

For the present situation under consideration, we can identify a characteristic time scale $\tau = \rho R_{avg}^2 / 8\mu$ defining the underlying phenomenology. At long time $t/\tau >> 1$, the resulting equation approximates to $\langle \xi^2 \rangle \approx (2u\tau)t$. In contrast to the single capillary dynamics [29], here the equation describes the ensemble behavior of random liquid motions in different possible directions through the isotropically distributed random capillaries constituting the paper matrix. Thus, the present notion bears an analogy with the molecular diffusion process due to random motions of the molecules [30]. Accordingly, we can ascribe the liquid propagation through paper as an effective diffusion process at late stage, given by $l^2 = Dt$, with D being the diffusivity, and l being the diffusion length. Here $D = 2u\tau = 2\left(2\sigma\cos\theta_0 / \rho R_{avg}\right)\left(\rho R_{avg}^2 / 8\mu\right) = R_{avg}\sigma\cos\theta_0 / 2\mu$. The other limit of early stage asymptote (at $t/\tau << 1$) describes $l^2 = (2u)t^2$, which conforms to the ballistic dynamics of liquid propagation.

It is important to mention that the diffusion dynamics obtained in our study eventually results in a Fickian diffusion process within the fibers. However, non-Fickian diffusion scenarios may also arise when the mean free path of the fluid molecules are of the order of the diameter of the microcapillary under consideration [31,32]. This is often seen in the microporous layer of a fuel cell electrode [31,32]. The present study, however, considers the transport of liquids, mostly aqueous solutions considered in paper based microfluidic applications. Under those circumstances, however, the mean free path of the fluid is much smaller than the diameter of paper microcapillaries (for example $10\,\mu m$ for Whatman grade 1 paper). Therefore, the liquid transport dynamics can be sufficiently represented by the above mentioned model consideration along with the possible overlap with the molecular dynamics, as shown here.

The simple dynamical analysis portrayed as above holds the capability of explaining a plethora of complex fluidic operations on a paper matrix. Some such examples are presented subsequently.

Liquid imbibition: In paper microfluidics, a liquid sample traverses through paper matrix. We cite a few pertinent experimental observations [18,33], and put these in

perspectives of the imbibition dynamics following the present paradigm (Fig. 2). According to our model, $l^2/D\tau$ appears to be a unique function of t/τ, irrespective of the system considered. The experimental observations appear to be consistent with this notion (Fig. 2). From the host of data, we consider a representative sample of the transport of water ($\rho = 10^3\,\mathrm{kg/m^3}$, $\mu = 10^{-3}\,\mathrm{Pa\text{-}s}$) through Whatman filter paper (grade 1) ($R_{avg} = 5.4\mu\mathrm{m}$). This shows $\tau = \rho R_{avg}^2/8\mu = 3.65\mu\mathrm{s}$ whereas the experiments are observed over the time scale of 100s. Thus, the usual experimental observations are well within the long time ($t/\tau >> 1$) asymptotic regime of diffusive dynamics $l^2 = Dt$).

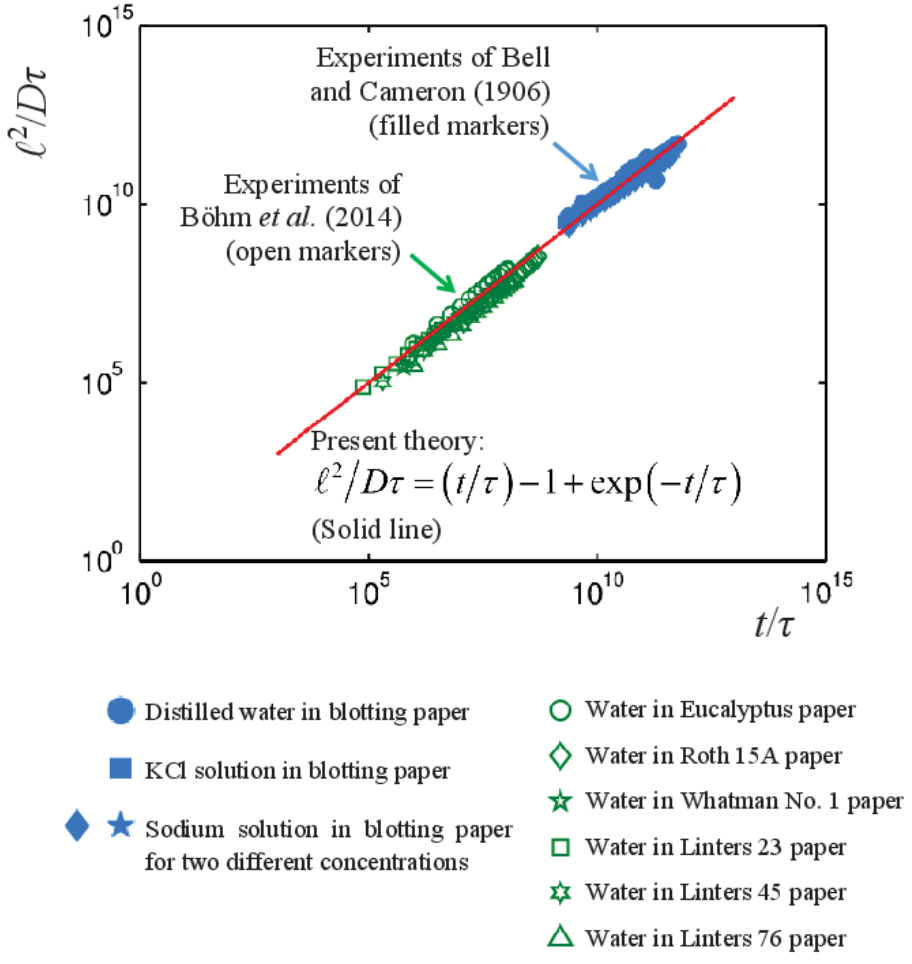

Fig. 2. Temporal progression of liquid fronts through paper matrix, following the present theory (solid line), as compared to reported experimental observations (markers) [18,33]. The thermophysical properties of the liquids, characteristics of the papers, and other physical parameters are in accordance with the Refs [18,19,33–38].

Mixing and separation of analytes: We next highlight the application of our model towards understanding the mixing and separation of analytes, while two adjacent liquid streams move parallel to each other through a paper matrix [39] (shown schematically in Fig. 3a, while looking at a paper strip from the top). Usually, microfluidic channels are designed on paper matrices with the boundaries marked with hydrophobic barriers. The barrier prevents leakage of liquid outside the domain under consideration. This is a paper based analogue of parallel stream lamination in microfluidic channel. Often Y shaped channels are considered for studying mixing.

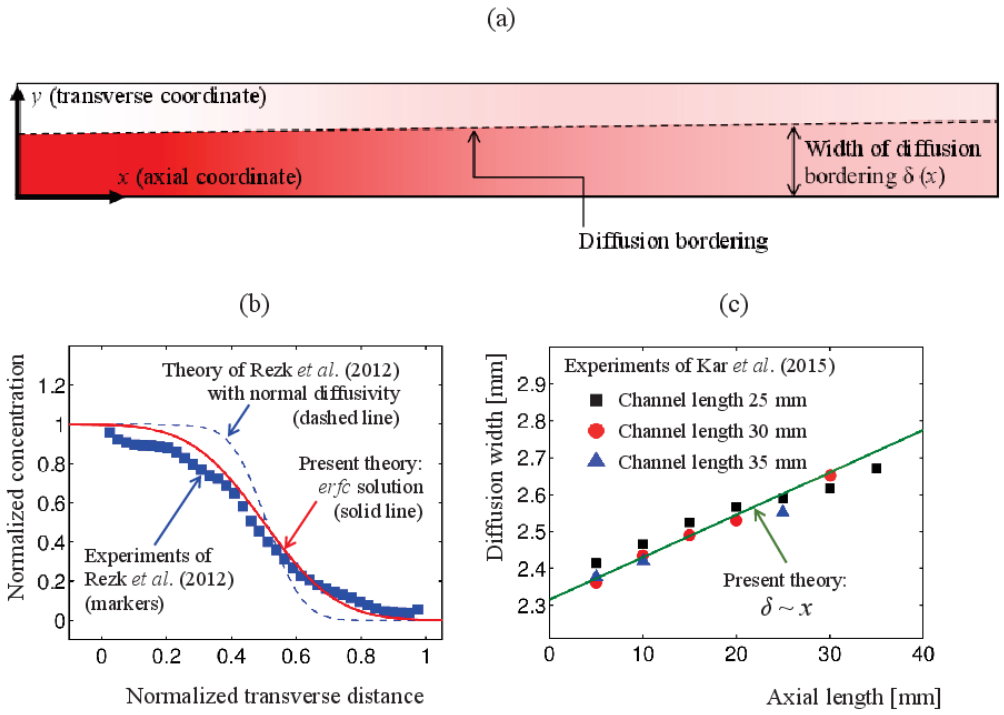

Fig. 3. Mixing and separation of analytes in a paper microfluidic channel. (a) A schematic representation of the situation, while looking at a paper strip from the top. Distributions of different fluids, introduced from the left edge, are shown in different shades. The diffusion bordering earmarks the region across which the concentration changes from one value to another due to diffusion. (b) Transverse distribution of concentration and comparison with Rezk *et al.* [40]. We consider normalized transverse distance $=4\left(y-0.5\right)$ in our model, in order to permit origin shifting for the sake of having common basis for comparison with Rezk *et al.* [40]. (c) Axial variations in the width of diffusion bordering. Experimental observations of Kar *et al.* [41] on blood plasma separation on paper-based devices are considered.

To comprehend the mixing characteristics, one can recall the diffusive transport equation for the concentration (C) distribution: $\mathbf{v}\cdot\nabla C=D\left(\partial^2 C/\partial y^2\right)$, where y

denote the transverse direction (cf. Fig. 3a). Here $\mathbf{v}$ denotes the velocity vector. It needs to be emphasized that the thickness of a paper is much less than its axial extents. Thus, liquid transport can be considered to be two-dimensional in nature. Diffusive transport between two parallel liquid streams in a paper matrix can be considered as flow along the x direction, with mixing along the transverse y direction. Thus, the above equation sufficiently retains the subtleties of parallel stream mixing behavior in paper matrix.

In a microchannel, mixing occurs due to diffusion during the parallel movement of two fluids in contact. However, for such situation, the axial advection dynamics (here considered along x direction) is also important, detailed elsewhere [42]. Considering $\mathbf{v} = (D/2x)\hat{\mathbf{e}}_x$, with $\hat{\mathbf{e}}_x$ being the unit vector along x direction, the diffusion equation transforms to $C_x = 2xC_{yy}$. This has the analytical solution: $C = 2^{-1}\,\mathrm{erfc}(\eta)$, where $\eta = y/2x$ is a coordinate invariant variable. This complementary error function based solution for concentration distribution is found to agree well with the reported experimental observation of Ref. [40] (Fig. 3b).

In Ref. [40], the diffusive transport and the consequent concentration distribution has been presented, considering uniform velocity and diffusivity based on the chosen liquid (dashed line in Fig. 3b). Thus, enhanced diffusivity consideration was needed to fit the experimental observation in their study. However, the present diffusive dynamics based notion of liquid transport through paper (solid line in Fig. 3b) agrees well with the experimental observations (markers in Fig. 3b), without any artificial fitting.

The definition of invariance $\eta = y/2x$ provides us an important aspect of the width δ of the diffusion bordering across the two-fluid interface (cf. schematic in Fig. 3a). The diffusion bordering earmarks the region across which the concentration changes from one value to another due to diffusion. Our analysis shows $\delta \sim x$ (see Fig. 3c), in sharp contrast to the notions $\delta \sim x^{1/2}$ or $\delta \sim x^{1/3}$ [42] near the centerline or near the wall, respectively, observed during the transverse diffusion in pressure driven flow. Therefore, for a given axial movement of the fluid, the lateral spread is more pronounced in the paper than that in a co-flow through microchannel. Other than mixing, the diffusive transport across two adjacent streams of liquids is also utilized

for separation of species suspended in the liquids [41] (markers in Fig. 3c). In this respect, use of paper channels provides rapid, portable, and low cost solution. The separation along the length of the channel can be realized through the present notion of $\delta \sim x$ (solid line in Fig. 3c).

Hydrodynamics of writing with ink: The hydrodynamics of ink flow and its distribution during writing by pen is an intriguing research question from fluid dynamics perspective [8]. When a pen moves with speed V_p over a paper surface, it leaves a trail of ink that spreads through the paper network and forms a line (Fig. 4). For quantitative depiction, a reference frame $\tilde{x}-\tilde{y}-\tilde{z}$ which remains fixed with respect to the ground can be considered. Following the present arguments, conceptualizing the ink spreading in terms of a diffusion process, the ink concentration C_{ink} distribution can be modeled as $\left(C_{ink}\right)_t = D\left(C_{ink}\right)_{\tilde{y}\tilde{y}}$. Now, we shift the coordinate to the $x-y-z$ frame that moves with the pen. The reference frames are connected through the relations $x=\tilde{x}+V_p t$, $y=\tilde{y}$ and $z=\tilde{z}$. This pertains to the transformed diffusion equation $V_p\left(C_{ink}\right)_x = D\left(C_{ink}\right)_{yy}$.

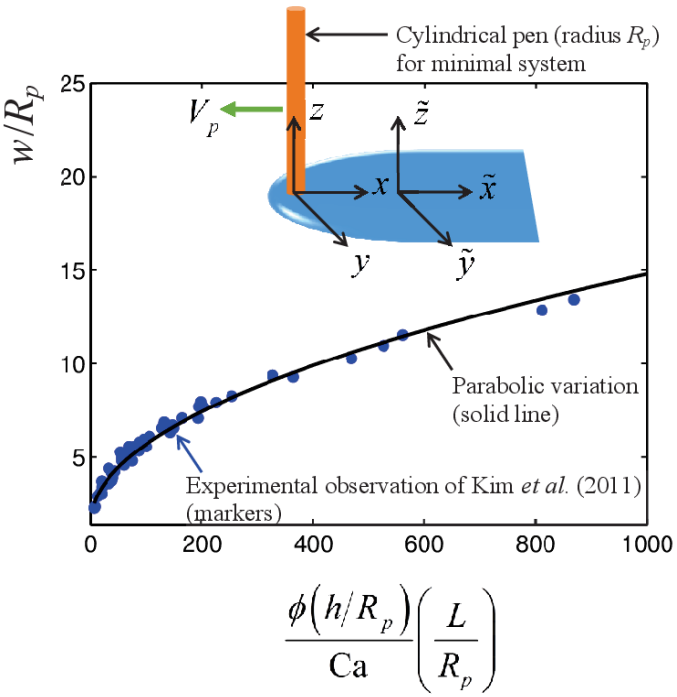

Fig. 4. Ink distribution during writing. Minimal system experimental observation (markers) of Kim *et al.* [8] is considered for describing the parabolic distribution (solid line) of ink around the pen. A schematic (exaggerated for better understanding) of the process is also presented for comprehension.

The above diffusion equation leads to the scaling relation $y^2 \sim Dx/V_p$ for the profile of the ink front around the tip of the pen. The present ensemble network based analysis provides us $D = R_{avg}\sigma\cos\theta_0/2\mu$. Compiling these, we obtain $y \sim \left(R_{avg}\cos\theta_0/2\right)^{1/2} x^{1/2}\,\mathrm{Ca}_p^{-1/2}$, a parabolic distribution of ink around the pen tip (cf. Fig. 4), where $\mathrm{Ca}_P = \mu V_p/\sigma$ is the capillary number of writing. Towards comprehending ink spread characteristics, experiments [8] had been performed with minimal system using a porous medium (having pillars of height h), and a cylindrical tube as a pen. The study [8] uncovers a universal scaling relation in the form of parabolic ink distribution $w \sim (\phi h)^{1/2} L^{1/2}\,\mathrm{Ca}_p^{-1/2}$ around the pen tip where w and L correspond to y and x in our model, and $\phi = (f-1)/f$ with f being the roughness defined as the actual surface area divided by the projected area. It is worth mentioning that the present notion on the diffusive transport of liquid through paper can unveil a similar facet, in agreement with the experimental finding (cf. Fig. 4).

To summarize, our study unveils that liquid transport through paper matrix, in elusively diverse applications, can be conceptualized through considerations of unique and generalized dynamical characteristics. Though the liquid flow through the single elementary microcapillary is governed by the capillary filling dynamics, the resultant behavior through all such capillaries resembles universal diffusive transport. This is attributable to the randomness in the distribution of the constituent fibers in a paper matrix. Diffusion based paradigm is found to rationalize various reported observations ranging from transport of liquid in paper based diagnostic devices to writing with ink on a paper platform.

SUPPLEMENTARY MATERIAL

See Supplemental Material, for the details regarding:

(i) Molecular kinetic viewpoint of wetting process considered in the present work.

(ii) Details of the micro-particle image velocimetry (μ-PIV) analysis considered in the present study.

ACKNOWLEDGEMENT

We gratefully acknowledge the financial support provided by the Indian Institute of Technology Kharagpur, India [Sanction Letter no.: IIT/SRIC/ATDC/CEM/2013-14/118, dated 19.12.2013] and The Royal Academy of Engineering, London, UK [HEPI\1516\27]. We also acknowledge the Council of Scientific and Industrial Research (CSIR), for providing fellowship to SK to carry out the research work.

REFERENCES

[1] S.R. Fischer, *History of Writing* (Reaktion Books, 2001).

[2] A. Gaur, *A History of Writing* (British Library, 1985).

[3] C.M. Cheng, A.W. Martinez, J. Gong, C.R. Mace, S.T. Phillips, E. Carrilho, K.A. Mirka, and G.M. Whitesides, Angew. Chemie - Int. Ed. **49**, 4771 (2010).

[4] A.W. Martinez, S.T. Phillips, M.J. Butte, and G.M. Whitesides, Angew. Chemie - Int. Ed. **46**, 1318 (2007).

[5] A.W. Martinez, S.T. Phillips, and G.M. Whitesides, Proc. Natl. Acad. Sci. U. S. A. **105**, 19606 (2008).

[6] S. Gruener, Z. Sadjadi, H.E. Hermes, a. V. Kityk, K. Knorr, S.U. Egelhaaf, H. Rieger, and P. Huber, Proc. Natl. Acad. Sci. **109**, 10245 (2012).

[7] R. Holtzman and E. Segre, Phys. Rev. Lett. **115**, 1 (2015).

[8] J. Kim, M.W. Moon, K.R. Lee, L. Mahadevan, and H.Y. Kim, Phys. Rev. Lett. **107**, 2 (2011).

[9] R. Kopelman, S. Parus, and J. Prasad, Phys. Rev. Lett. **56**, 1742 (1986).

[10] J. Cai, E. Perfect, C.L. Cheng, and X. Hu, Langmuir **30**, 5142 (2014).

[11] M. Reyssat, L. Courbin, E. Reyssat, and H.A. Stone, J. Fluid Mech. **615**, 335 (2008).

[12] H.S. Wiklund and T. Uesaka, Phys. Rev. E **87**, 1 (2013).

[13] O. Chepizhko and F. Peruani, Phys. Rev. Lett. **111**, 1 (2013).

[14] M. V Tamm, L.I. Nazarov, a a Gavrilov, and a V Chertovich, Phys. Rev. Lett. **114**, 1 (2015).

[15] S.C. Weber, A.J. Spakowitz, and J.A. Theriot, Phys. Rev. Lett. **104**, 27 (2010).

[16] A. Ashari, T.M. Bucher, H.V. Tafreshi, M.A. Tahir, and M.S.A. Rahman, Int. J. Heat Mass Transf. **53**, 1750 (2010).

[17] A.M.M. Rosa, A.F. Louro, S.A.M. Martins, J. Inácio, A.M. Azevedo, and D.M.F. Prazeres, Anal. Chem. **86**, 4340 (2014).

[18] A. Böhm, F. Carstens, C. Trieb, S. Schabel, and M. Biesalski, Microfluid. Nanofluidics **16**, 789 (2014).

[19] F.T.T. Carson, J. Res. Natl. Bur. Stand. (1934). **24**, 435 (1940).

[20] S. Guo, M. Gao, X. Xiong, Y.J. Wang, X. Wang, P. Sheng, and P. Tong, Phys. Rev. Lett. **111**, 1 (2013).

[21] S. Guo, C.H. Lee, P. Sheng, and P. Tong, Phys. Rev. E **91**, 1 (2015).

[22] M. Radiom, C. Yang, and W.K. Chan, Nanoscale Res. Lett. **8**, 282 (2013).

[23] C. Bakli and S. Chakraborty, Nano Lett. **15**, 7497 (2015).

[24] T.D. Blake, J. Colloid Interface Sci. **299**, 1 (2006).

[25] A.E. Kobryn and A. Kovalenko, J. Chem. Phys. **129**, (2008).

[26] C. Bakli and S. Chakraborty, Appl. Phys. Lett. **101**, (2012).

[27] T.D. Blake and J.M. Haynes, J. Colloid Interface Sci. **30**, 421 (1969).

[28] S. Das and S.K. Mitra, Phys. Rev. E **87**, 1 (2013).

[29] S. Das, P.R. Waghmare, and S.K. Mitra, Phys. Rev. E **86**, 1 (2012).

[30] E. Lutz, Phys. Rev. E **64**, 51106 (2001).

[31] L.M. Pant, S.K. Mitra, and M. Secanell, Int. J. Heat Mass Transf. **58**, 70 (2013).

[32] L.M. Pant, S.K. Mitra, and M. Secanell, J. Power Sources **206**, 153 (2012).

[33] J.M. Bell and F.K. Cameron, J. Phys. Chem. **50**, 658 (1906).

[34] V.A. Bloomfield and R.K.K. Dewan, J. Phys. Chem. **75**, 3113 (1971).

[35] J. Kestin, H.E. Khalifa, and R.J. Correia, J. Phys. Chem. Ref. Data **10**, 71 (1981).

[36] C.E. Grimes, J. Kestin, and H.E. Khalifa, J. Chem. Eng. Data **24**, 121 (1979).

[37] H.-L. Zhang and S.-J. Han, J. Chem. Eng. Data **41**, 516 (1996).

[38] K. Ali, A.-H.A. Shah, S. Bilal, and A.-H.A. Shahb, Colloids Surfaces A Physicochem. Eng. Asp. **337**, 194 (2009).

[39] J.L. Osborn, B. Lutz, E. Fu, P. Kauffman, D.Y. Stevens, and P. Yager, Lab Chip **10**, 2659 (2010).

[40] A.R. Rezk, A. Qi, J.R. Friend, W.H. Li, and L.Y. Yeo, Lab Chip **12**, 773 (2012).

[41] S. Kar, T.K. Maiti, and S. Chakraborty, Analyst **140**, 6473 (2015).

[42] R.F. Ismagilov, A.D. Stroock, P.J.A. Kenis, G. Whitesides, and H.A. Stone, Appl. Phys. Lett. **76**, 2376 (2000).